PAPER

Check for updates

Metallo-β-lactamases immobilized by magnetic zeolitic imidazolate frameworks-8 for degradation of β-lactam antibiotics in an aqueous environment†

Quanfang Wang,[a] Yuefeng Sun,[b] Shidi Zhao,[c] Chuqi Bai,[a] Zhiwei Cong,[d] Yalin Dong [ID] *[a] and Taotao Wang [ID] *[a]

Residual antibiotics in nature are an important cause of antimicrobial drug resistance, and how to deal with residual β-lactam antibiotics in aqueous environments has become an urgent issue. In this work, magnetic zeolitic imidazolate frameworks-8 (ZIF-8) for immobilizing metallo-β-lactamases (MBLs), or Fe_3O_4@ZIF-8@MBLs, were successfully synthesized using the one-pot method in aqueous solution. The morphology and chemical structure of Fe_3O_4@ZIF-8@MBLs were characterized by scanning electron microscopy, energy dispersive spectra, X-ray diffraction, infrared spectra, physical adsorption, and zeta potential. Further, the degradation performance of Fe_3O_4@ZIF-8@MBLs for β-lactam antibiotics (penicillin G, cefoperazone, meropenem) in an aqueous environment was investigated by UV-visible absorption spectrophotometry. The results indicated that Fe_3O_4@ZIF-8@MBLs, compared to control ZIF-8, exhibited superior degradation ability, excellent reusability, and better stability under several harsh conditions. The strategy of combining ZIF-8 and MBLs to form magnetic porous polymers may be suitable for removing β-lactam antibiotics from an aqueous environment. This work provided an original insight into future studies on the degradation of β-lactam antibiotics employing MBLs immobilized by magnetic metal–organic frameworks.

1. Introduction

The freshwater pollution caused by pharmaceutical and personal care products (PPCPs) has progressively emerged as a global environmental and public health concern.[1–3] Among the various types of PPCPs, antimicrobial residues are one of the most prevalent and account for a significant proportion of the water environment pollution,[4] which include macrolides, sulfonamides, quinolones, and tetracyclines.[5] Moreover, the expanded production and widespread utilization of β-lactam antibiotics[6,7] has led to the constant discharge from urban areas, hospitals, pharmaceutical manufacturers, and livestock industries. Studies have indicated that residual penicillins ranged from 3–48 ng L^{-1} in surface water,[8] while they could reach up to 1.67 μg L^{-1} in effluent discharged from sewage treatment plants.[9] In surface water and non-clinical wastewater,

the distribution of cephalosporins varied from 0.1–5000 ng L^{-1}.[10] The carbapenem antibiotic, meropenem, has not been detected in surface water yet, while effluent concentrations in wastewater treatment plants could reach 27–68 ng L^{-1}.[11] Pathogenic bacteria with long-term exposure to antibiotic residues can develop resistance *via* mobile genetic elements, enzymatic mechanisms, and conjugative plasmids,[12] further exacerbating the issue of antimicrobial resistance.[13]

Researchers have developed various advanced degradation techniques to treat PPCPs in recent years, such as physical adsorption, advanced oxidation process, and biotechnology.[14–16] Several primary methods for removing β-lactam antibiotics include activated sludge, UV oxidation, and biodegradation techniques. The activated sludge, mainly applied by manufacturers, cannot completely remove various types of antibiotics from wastewater,[17] and the oxidation process[18,19] is temporarily difficult to reach industrial-scale due to the high initial investment, complex treatment process, and demanding conditions required. By contrast, bio-enzymes are an ideal, efficient, low-cost, and environmentally friendly technology, which includes non-selective oxidative enzymes such as laccase[20] and specific lactam hydrolases. Several researchers were keen to combine the recoverability of magnetic nanoparticles with the specificity of β-lactamases to develop diverse forms of magnetically responsive composites for the degradation of antibiotics in water environments.[21–25] Fatima *et al.*[21] immobilized β-

[a]*Department of Pharmacy, The First Affiliated Hospital of Xi'an Jiaotong University, Xi'an 710061, China. E-mail: wangtaotao1989@mail.xjtu.edu.cn; dongyalin@mail.xjtu.edu.cn*

[b]*School of Pharmacy, Xi'an Medical College, Xi'an 710021, China*

[c]*Precision Medicine Center, The First Affiliated Hospital of Xi'an Jiaotong University, Xi'an 710061, China*

[d]*School of Mechanical Engineering, Xi'an Jiaotong University, Xi'an 710049, China*

lactamase from *Bacillus tropicalis* EMB20 on Fe_3O_4 magnetic nanoparticles and further used them for the efficient remediation of meropenem. The nanoconjugates retained up to 57% of their initial activity after 5 consecutive cycles of repeated use. The study by Gao et al.[22] was even more appealing. They reused β-lactamase immobilized on SiO_2-coated Fe_3O_4 nanoparticles 35 times, and the degradation efficiency remained above 95%. Shokoohizadeh et al.[23] immobilized the metallo-β-lactamase, IMP-1, on Fe_3O_4 magnetic nanoparticles coated with SiO_2 shell, and the immobilized enzymes retained 80% of their activity after 15 reaction cycles. Overall, the above studies present an effective and reusable method for degrading antibiotics from wastewater.

Metal–organic frameworks (MOF) are porous materials with a periodic network structure formed by self-assembly, and because of their large specific surface area and good stability, MOF are widely used in many fields.[26] Researchers have been able to utilize the excellent adsorption properties of MOF to degrade a variety of antimicrobial drugs in the aqueous environment.[27–31] Besides, MOF can also provide a suitable microenvironment to immobilize the enzyme, whose activity and stability are significantly enhanced.[32] Zeolitic imidazolate frameworks-8 (ZIF-8), formed by divalent zinc ions and imidazole ring, are the most representative class of zeolitic imidazolate frameworks.[33] Paula et al.[31] demonstrated that upon contact of the β-lactam antibiotics with the zinc-containing skeleton of ZIF-8, cleavage of the four-membered β-lactam ring occurs, leading to the degradation of the antibiotics. Yang et al.[34] encapsulated penicillinase into ZIF-8 by a self-assembly method and investigated the catalytic performance of β-lactamase@ZIF-8 for degrading penicillins. Their results suggested that the catalytic activity of the immobilized enzyme was significantly enhanced over the free enzyme and showed superior stability under a variety of conditions, including high temperature, organic solvents, and enzyme inhibitors. Hao and coworkers[35] encapsulated cephalosporinase (AmpC) and Prussian blue (PB) into ZIF-8, thereby preparing an AmpC/PB@ZIF-8 MOF nanocatalyst with photothermal properties for efficient catalytic degradation of cephalosporins.

Herein, Fe_3O_4@ZIF-8@MBLs were successfully synthesized in an aqueous solvent and characterized by scanning electron microscopy, energy dispersive spectra, X-ray diffraction, infrared spectra, physical adsorption, and zeta potential. The typical β-lactam antibiotics were selected as substrates, and the degradation performance and reusability of ZIF-8 and Fe_3O_4@ZIF-8@MBLs were investigated. Then the stability was evaluated after incubation at different temperatures, pH, and enzyme inhibitors. The synthesized Fe_3O_4@ZIF-8@MBLs were proven to be one of the promising strategies for degrading β-lactam antibiotics in the water environment.

2. Experimental

2.1 Chemicals and reagents

Metallo-β-lactamases (MBLs) were purchased from Junfeng Bioengineering (Hangzhou, China), which were expressed in recombinant *E. coli*. Penicillin G (PG, 1650 U mg^{-1}),

cefoperazone (CEF, 98%), meropenem (MER, 98%), zinc chloride (99%), and sodium hydroxide (99%) were purchased from Macklin (Shanghai, China). Monodispersed magnetite microspheres (Fe_3O_4–COOH, 300–400 nm), zinc acetate (99%), 2-methylimidazole (2-MIM, 98%), *N*-(3-dimethylaminopropyl)-*N'*-ethylcarbodiimide hydrochloride (EDC, 98%), and *N*-hydroxysuccinimide (NHS, 98%) were purchased from Aladdin (Shanghai, China). Hydrochloric acid (36.46%) was obtained from Kelong (Chengdu, China). Ethylene diamine tetraacetic acid (DETA, 99.5%) was obtained from Wolsen (Xi'an, China). Avibactam sodium (AVI, 99.92%) was obtained from MedChemExpress (New Jersey, USA). Phosphate buffered saline (powder) was obtained from Servicebio (Wuhan, China). Bradford protein assay kit was purchased from Beyotime (Shanghai, China). Water was purified with a Millipore Milli-Q system (Bedford, USA).

2.2 Synthesis of ZIF-8-based composites

2.2.1 ZIF-8 and ZIF-8@MBLs. ZIF-8@MBLs were synthesized according to a classical method.[36] Specifically, 1 mL of zinc acetate (20 mmol L^{-1}) containing 5 mg MBLs was mixed gently on a custom-made vertical mixer for 15 min. Then, 1 mL of 2-methylimidazole (1.4 mol L^{-1}) was added quickly and the mixture was blended well at room temperature for 8 h. The products were collected by centrifugation (13 000 rpm, 10 min), washed with deionized water, and dried under vacuum. As for ZIF-8, zinc acetate solution without MBLs was used, and the other steps were performed as above.

2.2.2 Fe_3O_4@ZIF-8@MBLs. At first, EDC and NHS were used to activate the carboxyl groups of Fe_3O_4 magnetite microspheres. Specifically, newly prepared 100 μL of EDC (in PBS, 10 mg mL^{-1}) and 100 μL of NHS (in PBS, 10 mg mL^{-1}) were added into the washed 100 μL of Fe_3O_4 (5 mg mL^{-1}), and the solution was then blended on a custom-made vertical mixer for 30 min. Subsequently, the activated magnetite microspheres were collected by an external magnet and redispersed in 1 mL of zinc acetate (20 mmol L^{-1}) containing 2.5, 5, and 10 mg MBLs, and the mixture was blended well for 15 min. After that, 1 mL of 2-methylimidazole (1.4 mol L^{-1}) was added quickly and the mixture was blended well at room temperature for 8 h. The products were collected by external magnets and centrifugation (13 000 rpm, 10 min), washed with deionized water, and dried under vacuum. Meanwhile, the supernatant was collected to calculate the enzyme concentration by the Bradford method[37] to determine the loading capacity and efficiency of the composites. The custom-made vertical mixer is a vertical turntable equipped with test tube racks, which allows the reaction solution to mix well without the larger mass of Fe_3O_4 microspheres sinking to the bottom of the test tube.

2.3 Characterization

The microstructure and chemical composition of ZIF-8-based composites were attained by a field emission scanning electron microscope (SEM, JEOL JSM-7000F) equipped with energy dispersive spectroscopy (EDS). The X-ray diffraction (XRD) patterns were acquired by an X-ray diffractometer (Bruker D8

Advanced) with Cu anode material in the 2θ range of 10–80°. The zeta potential was measured using a zeta-potential analyzer (Malvern Zetasizer ZSU3205). The infrared spectra were collected on a Fourier transform infrared spectroscope (Shimadzu FTIR-8400S). The surface areas and pore size distribution were analyzed with a high-performance adsorption analyzer (ASAP 2020 PLUS HD88). The β-lactam antibiotics in solution were quantified by a UV-visible spectrophotometer (YOKE T2600) with quartz micro cuvette. Enzyme concentration in the supernatant was determined on an automatic microplate reader (Agilent BioTek Synergy LX).

2.4 Degradation experiments

The hydrolytic activity of the free enzyme was first investigated. 200 μL of free MBLs (5 mg mL^{-1}) was added into 2 mL of appropriate concentrations of PG (125 mg L^{-1}), CEF (30 mg L^{-1}), and MER (30 mg L^{-1}), and the change in UV-visible absorbance was recorded in real-time within 3 min after rapid mixing. To explore the effect of Zn^{2+} concentration on the activity of free MBLs, 200 μL of free enzyme solution (5 mg mL^{-1}) with Zn^{2+} concentration of 0–100 mmol L^{-1} was prepared and incubated at room temperature for 60 min. Then, a series of MBLs solutions were respectively added to the appropriate concentration of CEF, and the change of absorbance was recorded within 3 min.

Then the degradation activity of ZIF-8 based composites was measured along the following lines. A moderate concentration of antibiotic solution was chosen as the substrate to react with free MBLs, ZIF-8, and Fe$_3$O$_4$@ZIF-8@MBLs and the change in UV-visible absorbance of the antibiotic was recorded after some time. By monitoring the degree of decrease in absorbance, the reduction of the antibiotic could be calculated in conjunction with the established standard curve (Beer–Lambert Law), which in turn allowed for comparison of the degradation activities of free MBLs, ZIF-8, and Fe$_3$O$_4$@ZIF-8@MBLs.

Specifically, the synthesized ZIF-8 and Fe$_3$O$_4$@ZIF-8@MBLs were rehydrated and added to appropriate concentrations of CEF (30 mg L^{-1}, 2 mL), and the UV-visible absorbance values at 0, 0.5, and 1 h were recorded. Before each absorbance measurement, a small amount of reaction solution needs to be centrifuged (13 000 rpm, 10 min) and filtered (0.22 μm). The changes in absorbance of CEF were recorded for seven consecutive rounds with the same procedure. All reactions were performed on a custom-made vertical mixer.

2.5 Stability and selectivity experiments

To evaluate the stability under different temperatures, the synthesized ZIF-8 and Fe$_3$O$_4$@ZIF-8@MBLs were rehydrated and incubated in solution with 25, 50, and 100 °C for 1 h, respectively. To evaluate the stability under different pH, the synthesized composites were rehydrated and incubated in solution at pH 5.0, 7.0, and 10.0 for 1 h, respectively. To evaluate the effect of different inhibitors on the degradation activity of the composites, the synthesized composites were rehydrated and incubated in EDTA and AVI solution (50 μM) for 1 h. Then, the pre-treated composites were separated out by centrifugation

and the degradation activity was evaluated with the procedures above. Finally, the degradation of the synthesized composites against different types of β-lactam antibiotics was further investigated.

3. Results and discussion

3.1 Preparation and characterization of ZIF-8-based composites

The amount of MBLs added is an essential variable in the synthesis of Fe$_3$O$_4$@ZIF-8@MBLs. The enzyme concentration of the centrifugal supernatant was determined by the Bradford method, and the results were presented in Table S1.† When the added MBLs were about 5 mg, there was maximum loading efficiency, so this variable was fixed in subsequent studies.

SEM was used to characterize the morphology and microstructure. The monodispersed magnetic microspheres were presented as homogeneous spheres with a particle size of about 300–400 nm (Fig. 1a). It is a more efficient and economical way to synthesize ZIF materials in the aqueous solvent.[38] The synthesized ZIF-8 using a proper molar ratio (2-MIM : Zn^{2+} = 70 : 1)[36] resulted in products that were mostly dodecahedral and the molecular sizes were close to 1 μm, while some smaller particles were also found (Fig. 1b), which were attributed to the high local 2-MIM concentration resulting in a higher nucleation rate. However, when 5 mg of MBLs was added, the frame volume of ZIF-8 was drastically reduced and showed a polyhedral shape with uneven size (Fig. 1c). The added MBLs could act as nucleation seeds and/or be incorporated by particle adhesion to help form ZIF-8 crystals,[39] thus leading to the absence of a regular dodecahedral shape on the one hand, and the formation of smaller MOF particles on the other. As for Fe$_3$O$_4$@ZIF-8@MBLs, the small-sized ZIF-8@MBLs would attach to the Fe$_3$O$_4$ surface through the bonding between the activated carboxyl groups and Zn^{2+} (Fig. 1d). Of course, it couldn't be excluded that the enzyme molecules were also directly immobilized on the carboxyl groups of Fe$_3$O$_4$ given the one-pot method was used in the synthesis process. Fig. S1a†

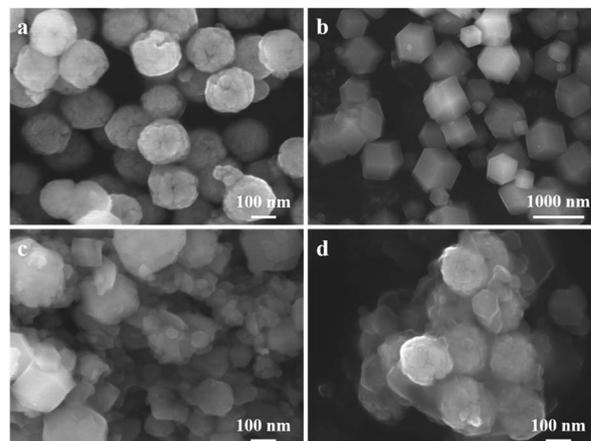Fig. 1 SEM images of Fe$_3$O$_4$ (a), ZIF-8 (b), ZIF-8@MBLs (c), and Fe$_3$O$_4$@ZIF-8@MBLs (d).

showed the EDS spectrum of Fe$_3$O$_4$@ZIF-8@MBLs, in which Fe, Zn, O, C, and Si were stably distributed, indicating that MBLs, ZIF-8, and Fe$_3$O$_4$ have been integrated into a composite system.

The XRD patterns of Fe$_3$O$_4$, ZIF-8, and Fe$_3$O$_4$@ZIF-8@MBLs were shown in Fig. 2a. All typical diffraction peaks of Fe$_3$O$_4$ and ZIF-8 crystal[40] were clearly shown and the diffraction angles of Fe$_3$O$_4$@ZIF-8@MBLs were mostly similar to that of ZIF-8, which indicated that the doping of Fe$_3$O$_4$ and MBLs would not destroy the original crystal framework structure of ZIF-8. Not surprisingly in FTIR (Fig. 2b), the stretching vibration of Zn–N bond (420 cm^{-1}) could be observed in both MBLs and ZIF-8. Multiple characteristic bands (C=N: 1583 cm^{-1}; C–N: 993 cm^{-1}, 1145 cm^{-1}; imidazole ring: 1350–1550 cm^{-1})[35] of ZIF-8 could be identified in Fe$_3$O$_4$@ZIF-8@MBLs. For Fe$_3$O$_4$@ZIF-8@MBLs, the weak band at 580 cm^{-1} was attributed to the Fe–O bond of Fe$_3$O$_4$.[41] The weak band at 2935 cm^{-1} and 1640 cm^{-1} could be ascribed to the stretching vibrations of the hydroxyl groups and the amide I band from MBLs, respectively, which confirmed that MBLs were successfully encapsulated in the framework of ZIF-8 and immobilized on the surface of Fe$_3$O$_4$.

As shown in Fig. 2c, the synthesized ZIF-8 and Fe$_3$O$_4$@ZIF-8@MBLs both exhibited typical I-type isotherms,[34,35,42] indicating the presence of a large number of microporous structures in these composites. The surface areas of ZIF-8 and Fe$_3$O$_4$@ZIF-8@MBLs were 935 m^2 g^{-1} and 838 m^2 g^{-1}, respectively, which illustrated that the encapsulation of MBLs slightly decreased the surface area of the ZIF-8. In addition, the average pore sizes of those composites were relatively close (ZIF-8: 1.9 nm; Fe$_3$O$_4$@ZIF-8@MBLs: 2.2 nm), further demonstrating that the doping of MBLs would not disrupt the microstructure of ZIF-8. Fig. 2d showed the zeta potential of each composite. Due to the doping of negatively charged MBLs (−18.5 mV) and Fe$_3$O$_4$ (−33.7 mV), the potential of Fe$_3$O$_4$@ZIF-8@MBLs (17.98 mV) was lower than that of ZIF-8 (37.8 mV), indicating that the MBLs and ZIF-8 frameworks have been formed *in situ* on the Fe$_3$O$_4$ microspheres. The above characterization results confirmed

that Fe$_3$O$_4$@ZIF-8@MBLs have been successfully prepared in this study.

3.2 Degradation performance

The UV-visible absorption methodology of each antibiotic was first developed. The PG, CEF, and MER were scanned at full wavelength (Fig. S2†) and the standard curves (Fig. S3†) were established by selecting the appropriate wavelength or local maximum absorption wavelength. Three linear fitted lines with $R^2 > 0.999$ were obtained for PG, CEF, and MER at 231 nm,[43] 265 nm, and 300 nm, respectively. Fig. 3a demonstrated the hydrolysis of PG, CEF, and MER by free MBLs within 3 min. Due to good dispersibility in solutions, the three β-lactam antibiotics were degraded in a very short period. The apparent hydrolysis rates of antibiotics were: MER > CEF > PG. Given the instability of meropenem in aqueous solutions, the cephalosporin antibiotic with a suitable degradation rate, CEF, was selected for the subsequent exploration. Although the catalysis of MBLs requires the participation of metal ions, excessive or insufficient metal ions could negatively affect the enzymatic activity,[44,45] not to mention that Zn^{2+} is the raw material for the synthesis of Fe$_3$O$_4$@ZIF-8@MBLs. Fig. 3b proved that Zn^{2+} at about 10 mmol L^{-1} in the synthetic solution significantly enhanced the enzyme activity compared to the addition of zinc ions at concentrations of 0 or 0.1 mmol L^{-1} (the instruction of the experimental MBLs states that 0.1 mmol L^{-1} Mg^{2+} and Zn^{2+} are important for enzyme action). Similar work can be found in the study of Li *et al.*[46]

In the first hydrolysis cycle for CEF, Fe$_3$O$_4$@ZIF-8@MBLs showed a better degradation activity (Fig. 3c). More importantly, it seemed that CEF didn't continue to be degraded much after 1 h, which was additional evidence that Fe$_3$O$_4$@ZIF-8@MBLs may be dual degradation mechanisms, including adsorption by ZIF-8 and hydrolysis by MBLs. However, it is difficult to determine antibiotics at relatively low
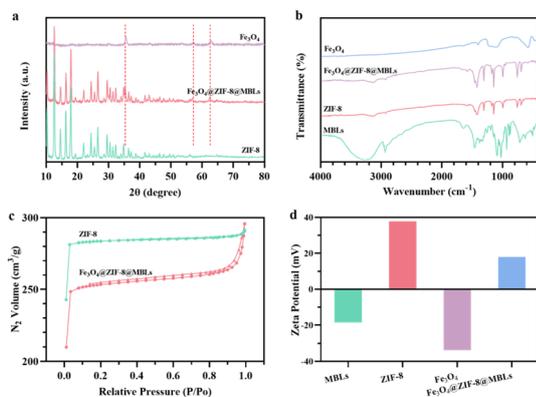

Fig. 2 The XRD patterns (a), FTIR spectra (b), N$_2$ adsorption (circles) – desorption (triangles) isotherms (c), and zeta potential (d) of ZIF, Fe$_3$O$_4$@ZIF-8@MBLs, and their raw materials. *P*, partial pressure of nitrogen. *P$_0$*, saturated vapor pressure of nitrogen.
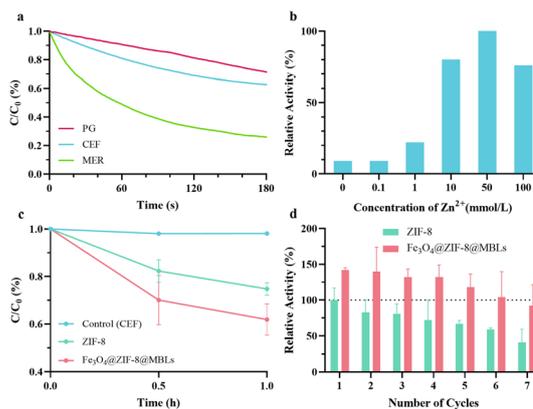

Fig. 3 (a) Remaining proportion of PG, CEF, and MER hydrolyzed by free MBLs within 3 min; (b) relative activity of free MBLs to hydrolyze CEF at different Zn^{2+} concentrations within 3 min; (c) remaining proportion of CEF degraded by ZIF-8 and Fe$_3$O$_4$@ZIF-8@MBLs within 1 h; (d) relative activity of ZIF-8 and Fe$_3$O$_4$@ZIF-8@MBLs to degrade CEF over 7 cycles. *C*, concentration of the antibiotic solution during the reaction. *C$_0$*, initial concentration of the antibiotic solution.

concentrations due to the limitations of UV-visible spectroscopy (Fig. S3†). For subsequent studies, it is necessary to establish more sensitive methods (*e.g.*, high-performance liquid chromatography) to explore the degradation performance of the ZIF-8 based composites under very low concentration conditions and demonstrate apparent kinetic parameters to argue for their utility in real wastewater environments.

Setting the ZIF-8 as a reference, the recyclability of two composites was next tested (Fig. 3d). The degradation ability demonstrated by Fe$_3$O$_4$@ZIF-8@MBLs (from 141.9% to 92.5%) was superior to that of ZIF-8 (from 100% to 40.9%) in the overall seven rounds, and this was one of the advantages of introducing Fe$_3$O$_4$ into composites. The decrease in the degradation ability of ZIF-8 and Fe$_3$O$_4$@ZIF-8@MBLs may be explained as the loss of composites or structural damage during the recovery process. Similar research demonstrated that the activity of Fe$_3$O$_4$@Cd-MOF@CS for catalytic degradation of penicillins could retain 62.07% after 5 cycles of reuse.[30]

3.3 Stability and selectivity

To visually compare the stability of ZIF-8 and Fe$_3$O$_4$@ZIF-8@MBLs, pretreatments with different temperatures, pH, and enzyme inhibitors within 1 h were performed, and the degradation activity was quantified by the change in antibiotic concentration (Fig. 4a–c). ZIF-8 itself exhibited promising catalytic properties after a series of treatments. It has been demonstrated that the degradation activity of ZIF-8 towards β-lactam antibiotics was attributed to the presence of Zn^{2+}, similar to the mononuclear and binuclear MBLs.[31] This present study further illustrated this idea and tentatively envisaged ZIF-8 to act as a more stable mimetic enzyme. Moreover, the mesoporous cavity of ZIF-8 could restrict the structural changes of enzyme molecules and thus maintain their activity. The degradation of Fe$_3$O$_4$@ZIF-8@MBLs was the result of the synergistic effect of MBLs and ZIF-8,[34] though the degradation activity of MBLs and ZIF-8 cannot be simply linearly superimposed.

Fe$_3$O$_4$@ZIF-8@MBLs showed undesirable degradation properties at high temperatures (Fig. 4a), and this may be due to enzyme inactivation caused by high temperatures as shown in Fig. S4a.† Besides, this work showed a low degradation activity of ZIF-8 based composites after incubation in acidic and alkaline conditions (Fig. 4b), elaborating by Saghir *et al.*[47] as the effect of charge surface of the adsorbent and adsorbate related to the pH of the solution. It is reported that MBLs were more sensitive to acidic conditions,[23,48] while Fe$_3$O$_4$@ZIF-8@MBLs still showed good degradation activity after 1 h incubation at pH 5.0. And this was another advantage of introducing Fe$_3$O$_4$ magnetic nanoparticles, in which the magnetic nanoparticles with large particle size could improve the stability of MOF-immobilized MBLs. When the free MBLs were inhibited by DETA (Fig. S4b†), the two composites, especially Fe$_3$O$_4$@ZIF-8@MBLs, exhibited excellent degradation activity (Fig. 4c).

The two ZIF-8 based composites exhibited a certain degree of selectivity towards the substrate (Fig. 4d and S2b–d†).[34] Within 1 h, the strongest apparent degradation effect was observed for MER, followed by PG and CEF. As for PG, however, the activity of ZIF-8 would be stronger compared to Fe$_3$O$_4$@ZIF-8@MBLs. This may be because the slowest apparent hydrolytic rate of the free MBLs against PG (Fig. 3a) rather affected the overall degradation activity of Fe$_3$O$_4$@ZIF-8@MBLs. Also, the difference in absorbance in the full wavelength scan spectrum before and after antibiotic degradation at the measured wavelengths could illustrate this (Fig. S2†). If an assay without chromatographic separation (such as the UV-vis spectrometry) is used to determine the reduction of antibiotics, it is important to select an appropriate detection wavelength (not the local maximum absorption wavelength of the antibiotic), which is one of the limitations of this study. Unfortunately, there is still a lack of research to further elucidate the internal mechanisms of antibiotic degradation by ZIF-8@MBLs. Our works provided some original insights for subsequent practical investigations on the degradation of β-lactam antibiotics using magnetic MOF-immobilized MBLs.

4. Conclusions

Fe$_3$O$_4$@ZIF-8@MBLs were successfully synthesized and characterized in this study, and the degradation performance of the composites against β-lactam antibiotics was investigated by UV-visible absorption spectrophotometry. The results showed that Fe$_3$O$_4$@ZIF-8@MBLs displayed very exceptional degradation ability, superior reusability, and high stability under harsh conditions. More research in the future is needed to further improve the overall performance of ZIF-8-based composites and to explore their catalytic degradation mechanisms. In conclusion, this work presents a promising strategy to deal with β-lactam antibiotic residues in the water environment.

Author contributions

Conceptualization, Y. D., T. W. and Q. W.; methodology, T. W., Q. W. and Z. C.; investigation, Q. W., Y. S. and S. Z.; data curation, Y. S. and S. Z.; writing—original draft preparation,
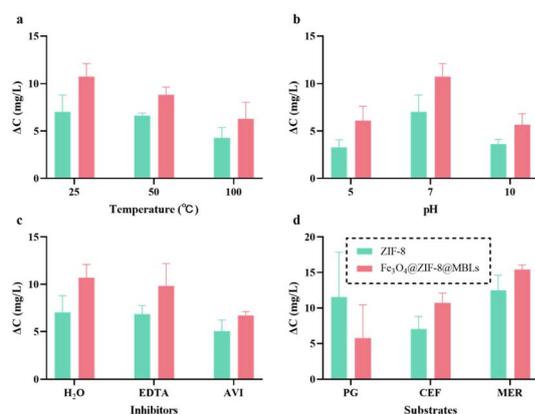

Fig. 4 Change in concentration of CEF (2 mL) degraded by ZIF-8 and Fe$_3$O$_4$@ZIF-8@MBLs within 1 h after treatment with different temperatures (a), pH (b), and enzyme inhibitors (c); change in concentration of PG, CEF, and MER (2 mL) degraded by ZIF-8 and Fe$_3$O$_4$@ZIF-8@MBLs within 1 h (d).

Q. W. and Y. S.; writing—review and editing, Y. D., T. W. and Q. W.; visualization, Q. W., S. Z. and C. B.; supervision, Y. D. and T. W.; all authors have read and agreed to the published version of the manuscript.

Conflicts of interest

There are no conflicts to declare.

Notes and references

1 A. S. Adeleye, J. Xue, Y. Zhao, A. A. Taylor, J. E. Zenobio, Y. Sun, Z. Han, O. A. Salawu and Y. Zhu, *J. Hazard. Mater.*, 2022, **424**, 127284.

2 L. Cizmas, V. K. Sharma, C. M. Gray and T. J. McDonald, *Environ. Chem. Lett.*, 2015, **13**, 381–394.

3 J. Wilkinson, P. S. Hooda, J. Barker, S. Barton and J. Swinden, *Environ. Pollut.*, 2017, **231**, 954–970.

4 Z. Wang, X. H. Zhang, Y. Huang and H. Wang, *Environ. Pollut.*, 2015, **204**, 223–232.

5 J. Wang, L. Chu, L. Wojnarovits and E. Takacs, *Sci. Total Environ.*, 2020, **744**, 140997.

6 H. Wushouer, Y. Tian, X. D. Guan, S. Han and L. W. Shi, *PLoS One*, 2017, **12**, e0190314.

7 J. S. Kanu, M. Khogali, K. Hann, W. Tao, S. Barlatt, J. Komeh, J. Johnson, M. Sesay, M. A. Vandi, H. Tweya, C. Timire, O. T. Abiri, F. Thomas, A. Sankoh-Hughes, B. Molleh, A. Maruta and A. D. Harries, *Trop. Med. Infect. Dis.*, 2021, **6**, 77.

8 K. Kummerer, *Chemosphere*, 2009, **75**, 417–434.

9 T. B. Minh, H. W. Leung, I. H. Loi, W. H. Chan, M. K. So, J. Q. Mao, D. Choi, J. C. Lam, G. Zheng, M. Martin, J. H. Lee, P. K. Lam and B. J. Richardson, *Mar. Pollut. Bull.*, 2009, **58**, 1052–1062.

10 E. Ali Noman, A. Al-Gheethi, R. M. Saphira Radin Mohamed, B. A. Talip, M. S. Hossain, W. Ali Hamood Altowayti and N. Ismail, *J. Hazard. Mater.*, 2021, **417**, 126040.

11 N. H. Tran, H. Chen, T. V. Do, M. Reinhard, H. H. Ngo, Y. He and K. Y. Gin, *Talanta*, 2016, **159**, 163–173.

12 P. Chaturvedi, P. Shukla, B. S. Giri, P. Chowdhary, R. Chandra, P. Gupta and A. Pandey, *Environ. Res.*, 2021, **194**, 110664.

13 C. J. L. Murray, K. S. Ikuta, F. Sharara, L. Swetschinski, G. Robles Aguilar, A. Gray, C. Han, C. Bisignano, P. Rao, E. Wool, S. C. Johnson, A. J. Browne, M. G. Chipeta, F. Fell, S. Hackett, G. Haines-Woodhouse, B. H. Kashef Hamadani, E. A. P. Kumaran, B. McManigal, S. Achalapong, R. Agarwal, S. Akech, S. Albertson, J. Amuasi, J. Andrews, A. Aravkin, E. Ashley, F.-X. Babin, F. Bailey, S. Baker, B. Basnyat, A. Bekker, R. Bender, J. A. Berkley, A. Bethou, J. Bielicki, S. Boonkasidecha, J. Bukosia, C. Carvalheiro, C. Castañeda-Orjuela, V. Chansamouth, S. Chaurasia, S. Chiurchiù, F. Chowdhury, R. Clotaire Donatien, A. J. Cook, B. Cooper, T. R. Cressey, E. Criollo-Mora, M. Cunningham, S. Darboe, N. P. J. Day, M. De Luca, K. Dokova, A. Dramowski, S. J. Dunachie, T. Duong Bich, T. Eckmanns, D. Eibach, A. Emami, N. Feasey, N. Fisher-Pearson, K. Forrest, C. Garcia, D. Garrett, P. Gastmeier, A. Z. Giref, R. C. Greer, V. Gupta, S. Haller, A. Haselbeck, S. I. Hay, M. Holm, S. Hopkins, Y. Hsia, K. C. Iregbu, J. Jacobs, D. Jarovsky, F. Javanmardi, A. W. J. Jenney, M. Khorana, S. Khusuwan, N. Kissoon, E. Kobeissi, T. Kostyanev, F. Krapp, R. Krumkamp, A. Kumar, H. H. Kyu, C. Lim, K. Lim, D. Limmathurotsakul, M. J. Loftus, M. Lunn, J. Ma, A. Manoharan, F. Marks, J. May, M. Mayxay, N. Mturi, T. Munera-Huertas, P. Musicha, L. A. Musila, M. M. Mussi-Pinhata, R. N. Naidu, T. Nakamura, R. Nanavati, S. Nangia, P. Newton, C. Ngoun, A. Novotney, D. Nwakanma, C. W. Obiero, T. J. Ochoa, A. Olivas-Martinez, P. Olliaro, E. Ooko, E. Ortiz-Brizuela, P. Ounchanum, G. D. Pak, J. L. Paredes, A. Y. Peleg, C. Perrone, T. Phe, K. Phommasone, N. Plakkal, A. Ponce-de-Leon, M. Raad, T. Ramdin, S. Rattanavong, A. Riddell, T. Roberts, J. V. Robotham, A. Roca, V. D. Rosenthal, K. E. Rudd, N. Russell, H. S. Sader, W. Saengchan, J. Schnall, J. A. G. Scott, S. Seekaew, M. Sharland, M. Shivamallappa, J. Sifuentes-Osornio, A. J. Simpson, N. Steenkeste, A. J. Stewardson, T. Stoeva, N. Tasak, A. Thaiprakong, G. Thwaites, C. Tigoi, C. Turner, P. Turner, H. R. van Doorn, S. Velaphi, A. Vongpradith, M. Vongsouvath, H. Vu, T. Walsh, J. L. Walson, S. Waner, T. Wangrangsimakul, P. Wannapinij, T. Wozniak, T. E. M. W. Young Sharma, K. C. Yu, P. Zheng, B. Sartorius, A. D. Lopez, A. Stergachis, C. Moore, C. Dolecek and M. Naghavi, *Lancet*, 2022, **399**, 629–655.

14 Y. Xu, T. J. Liu, Y. Zhang, F. Ge, R. M. Steel and L. Y. Sun, *J. Mater. Chem. A*, 2017, **5**, 12001–12014.

15 Y. Yang, Y. S. Ok, K. H. Kim, E. E. Kwon and Y. F. Tsang, *Sci. Total Environ.*, 2017, **596–597**, 303–320.

16 C. O. Okoye, R. Nyaruaba, R. E. Ita, S. U. Okon, C. I. Addey, C. C. Ebido, A. O. Opabunmi, E. S. Okeke and K. I. Chukwudozie, *Environ. Toxicol. Pharmacol.*, 2022, **96**, 103995.

17 C. X. Chen, A. Aris, E. L. Yong and Z. Z. Noor, *Environ. Sci. Pollut. Res. Int.*, 2022, **29**, 4787–4802.

18 X. He, S. P. Mezyk, I. Michael, D. Fatta-Kassinos and D. D. Dionysiou, *J. Hazard. Mater.*, 2014, **279**, 375–383.

19 J. H. Pereira, A. C. Reis, V. Homem, J. A. Silva, A. Alves, M. T. Borges, R. A. Boaventura, V. J. Vilar and O. C. Nunes, *Water Res.*, 2014, **65**, 307–320.

20 C. Zhang, S. You, J. Zhang, W. Qi, R. Su and Z. He, *Bioresour. Technol.*, 2020, **308**, 123271.

21 H. Fatima, A. Bhattacharya and S. K. Khare, *J. Environ. Manage.*, 2023, **329**, 117054.

22 X. J. Gao, X. J. Fan, X. P. Chen and Z. Q. Ge, *Int. J. Environ. Sci. Technol.*, 2018, **15**, 2203–2212.

23 M. J. Shokoohizadeh, A. Almasi, F. Karami, S. A. Mousavi and R. Khodarahmi, *Water Sci. Technol.*, 2022, **85**, 2189–2207.

24 S. C. Tsang, C. H. Yu, X. Gao and K. Tam, *J. Phys. Chem. B*, 2006, **110**, 16914–16922.

25 X. Gao, K. M. Yu, K. Y. Tam and S. C. Tsang, *Chem. Commun.*, 2003, 2998–2999, DOI: **10.1039/b310435d**.

26 H. Furukawa, K. E. Cordova, M. O'Keeffe and O. M. Yaghi, *Science*, 2013, **341**, 1230444.

27 G. Wu, J. Ma, S. Li, J. Guan, B. Jiang, L. Wang, J. Li, X. Wang and L. Chen, *J. Colloid Interface Sci.*, 2018, **528**, 360–371.

28 M. L. Wang, Z. Zhao, S. Lin, M. Su, B. Liang and S. X. Liang, *Environ. Sci. Pollut. Res.*, 2022, **29**, 50177–50191.

29 D. Sheng, X. Ying, R. Li, S. Cheng, C. Zhang, W. Dong and X. Pan, *Chemosphere*, 2022, **308**, 136249.

30 M. Pooresmaeil and H. Namazi, *Int. J. Biol. Macromol.*, 2021, **191**, 108–117.

31 M. V. Paula, A. L. Barros, K. A. Wanderley, G. F. de Sa, M. Eberlin, T. A. Soares and S. Alves, *J. Braz. Chem. Soc.*, 2018, **29**, 2127–2136.

32 J. J. Li, L. Yin, Z. F. Wang, Y. C. Jing, Z. L. Jiang, Y. Ding and H. S. Wang, *Chem. – Asian J.*, 2022, **17**, e202200751.

33 H. Dai, X. Z. Yuan, L. B. Jiang, H. Wang, J. Zhang, J. J. Zhang and T. Xiong, *Coord. Chem. Rev.*, 2021, **441**, 213985.

34 L. Yang, D. Hu, H. Liu, X. Wang, Y. Liu, Q. Xia, S. Deng, Y. Hao, Y. Jin and M. Xie, *J. Hazard. Mater.*, 2021, **414**, 125549.

35 Y. Hao, S. Deng, R. Wang, Q. Xia, K. Zhang, X. Wang, H. Liu, Y. Liu, M. Huang and M. Xie, *J. Hazard. Mater.*, 2022, **429**, 128294.

36 W. H. Chen, M. Vazquez-Gonzalez, A. Zoabi, R. Abu-Reziq and I. Willner, *Nat. Catal.*, 2018, **1**, 689–695.

37 M. M. Bradford, *Anal. Biochem.*, 1976, **72**, 248–254.

38 Y. Pan, Y. Liu, G. Zeng, L. Zhao and Z. Lai, *Chem. Commun.*, 2011, **47**, 2071–2073.

39 B. P. Carpenter, A. R. Talosig, J. T. Mulvey, J. G. Merham, J. Esquivel, B. Rose, A. F. Ogata, D. A. Fishman and J. P. Patterson, *Chem. Mater.*, 2022, **34**, 8336–8344.

40 H. C. Liu, L. G. Chen and J. Ding, *Microchim. Acta*, 2017, **184**, 4091–4098.

41 J. Du, X. Chen, K. Liu, D. Zhao and Y. Bai, *Sens. Actuators, B*, 2022, **360**, 131654.

42 X. Jiang, S. Su, J. T. Rao, S. J. Li, T. Lei, H. P. Bai, S. X. Wang and X. J. Yang, *J. Environ. Chem. Eng.*, 2021, **9**, 105959.

43 L. Tao, C. Zhiben and C. Xiaoying, *J. China Pharm. Univ.*, 1990, 211–214.

44 P. W. Thomas, M. Zheng, S. Wu, H. Guo, D. Liu, D. Xu and W. Fast, *Biochemistry*, 2011, **50**, 10102–10113.

45 R. Edwards, P. S. Hashmi and D. Greenwood, *J. Med. Microbiol.*, 1997, **46**, 807–809.

46 T. Li, Q. Wang, F. H. Chen, X. Li, S. Luo, H. L. Fang, D. H. Wang, Z. Li, X. J. Hou and H. Wang, *PLoS One*, 2013, **8**, e61914.

47 S. Saghir and Z. Xiao, *Mater. Res. Bull.*, 2021, **141**, 111372.

48 S. R. Schlesinger, S. G. Kim, J.-S. Lee and S.-K. Kim, *Biotechnol. Lett.*, 2011, **33**, 1417–1422.